



The Role of Polyethylene Glycol in Pore Diameter Modulation in Depth in p-Type Silicon

E. Ossei-Wusu,* J. Carstensen, E. Quiroga-González, M. Amirmaleki, and H. Föll^z

Institute for Materials Science, Christian-Albrechts-University of Kiel, D-24143 Kiel, Germany

The possibility of local modulation of the macropore diameter has been investigated for macropores at different pore depths on pre-patterned low-doped p-type silicon (p-Si) substrates. Using electrolytes based on HF/organic solvents, it is relatively easier to vary the diameter of deep pores compared to shallow pores. Adding polyethylene glycol to the electrolyte helps to achieve pore diameter modulation even at shallow depths. Using fast Fourier transform impedance spectroscopy (FFT IS), the pore growth was analyzed in-situ. A simple model was used to fit all the measured data, and some electrochemical parameters could be quantified. Comparing these parameters with the pore morphologies, it was observed that diffusion limitation is essential for achieving pore diameter modulation in p-Si by changing the applied current density.

© 2013 The Electrochemical Society. [DOI: [10.1149/2.020305jss](https://doi.org/10.1149/2.020305jss)] All rights reserved.

Manuscript submitted February 14, 2013; revised manuscript received March 20, 2013. Published April 4, 2013. This was Paper 2366 presented at the Honolulu, Hawaii, Meeting of the Society, October 7–12, 2012.

Since the discovery of electrochemically etched macropores in {100} oriented n-type silicon (n-Si) surfaces using back side illumination (bsi) in 1990 by Lehmann and Foell,¹ various morphologies and/or etch directions of the porous structures have been investigated.^{2–6} The pore morphology investigations are mostly centered on the variation of the pore diameter. Depending on the parameters, e.g. current density, HF concentration, substrate orientation, and doping concentration, the variation of the pore diameter can be either self-induced⁷ (where different modes of transitions between pore types were observed) or externally enforced.^{2,4,8}

With respect to enforced pore diameter modulation, it was reported in² that the diameters of n-Si macropores could be modulated by sinusoidal variation of the current density or the illumination intensity. This was expected since pore etching in n-Si fully obeys the well-known and accepted “space charge region” (SCR) model,¹ which states that the pore diameter is determined by the critical current density j_{PSL} at the pore tips. Matthias et al.⁹ used this concept to improve the modulation process and to extend it to smaller pore diameters. In their work they modulated not only the current density but also the etch potential in a complex way to overcome instability issues for the pore growth. They claimed that modulating the applied potential will let the SCR adjust itself and focus the holes to the pore tips allowing the pore etching process to follow the current density directly. With respect to the shape or profile of the modulated pores, it was reported in¹⁰ that it does not necessarily follow the modulation profile of the illumination intensity. A triangular illumination intensity modulation profile plus a quite different potential modulation was necessary to achieve the desired sinusoidal pore diameter variation which emphasizes, that even pore diameter modulation in n-Si, using back side illumination with several accessible parameters for controlling pore properties, can be a difficult task.

In strong contrast to n-Si pores, etching macropores into p-type silicon (p-Si) does not rely exclusively on the SCR model. After the discovery of p-Si macropores,¹¹ several models have been proposed for explaining the etching mechanism.^{12–14} A recent model of the authors in¹⁵ emphasizes the amount of water in the electrolyte since that is tied to the oxidation of Si. Due to the complex nature of the p-Si macropores etching, not much research work has been done on this substrate type compared to the popularity n-Si enjoys. The effect of the current on the p-Si pore geometry was investigated in,¹⁶ where it was observed that a change in the current density primarily changed the etching rate and thus not noticeably the pore diameter. In,¹⁷ Kochergin and Foell argued that modulating the current density has “no” effect on the pore diameter because pores always grow to a diameter that produces field-free Si between the pores. They assumed that large amplitude modulations might be the key but emphasized that this

was just a speculation. In¹⁸ however, electrochemically etched p-Si macropores with modulated diameters were demonstrated and used to make freestanding arrays of silicon wires intended as anodes for Li-ion batteries. The principle behind the pore diameter modulation was not explained.

As it will be discussed in this paper, the reason for the partly contradictory results in the literature is related to the strong dependence of p-Si pore etching on slight variation of etching conditions (much stronger than for n-Si), like doping, additives to the electrolyte and the existence, pitch, and arrangement of pore pre-patterning structures. In this paper we investigate the fundamental effect of the current density variation on the pore diameters at different depths using HF/DMF electrolytes on pre-patterned low-doped p-Si samples. It will also be demonstrated that the use of surfactants such as polyethylene glycol (PEG) is very helpful for pore diameter modulation in p-Si. While scanning electron microscopy (SEM) was used to characterize the “post-mortem” pore morphology, fast Fourier transform (FFT) impedance spectra (IS), taken every 2 s, were used to obtain in-situ information. The measured spectra were analyzed and the resulting parameter changes with pore depth compared to the pore morphologies.

Experimental

Macropores were electrochemically etched into mono-crystalline boron-doped p-Si with {100} orientation, a nominal resistivity of 20 Ωcm (10^{14} cm^{-3} doping concentration), and back side aluminum metallization for good ohmic contacts. This is the standard p-Si substrate typically used to etch “good” macropores. For uniform pore diameter variations, and to ensure that IS data mirror single pore parameters and do not just give an average over geometrically different pores, it is necessary to pre-pattern the starting material as e.g. reported in^{2,9} for n-Si. In our investigation the p-Si substrates were photo-lithographically pre-structured followed by KOH etching¹⁸ resulting in a simple cubic lattice of inverted pyramids with a spacing of 2 to 3 μm , serving as nuclei for the pores. The wafers were cut into 2×2 cm^2 pieces for the pore etching with an effective etching area of 1 cm^2 . Etching was performed at a controlled temperature of 20°C. The electrolytes were prepared from HF (48 wt%) and DMF in the ratio 1:10.

In another set of experiments, the surfactant PEG (3400) was added to the electrolyte and the results were compared to the pores etched without PEG. Note that PEG was chosen because it is known to increase both the electrolyte viscosity and the surface passivation. Electrolytes without PEG will be indicated only as HF/DMF; where PEG was added, it will be written as HF/DMF (PEG). The concentration of the PEG was 0.011 M. To modulate the pore diameter the current density was alternated between 19 mA/cm^2 and 3 mA/cm^2 in a step-like manner for different etching times after different time of pore etching.

*Electrochemical Society Student Member.

^zE-mail: hf@tf.uni-kiel.de

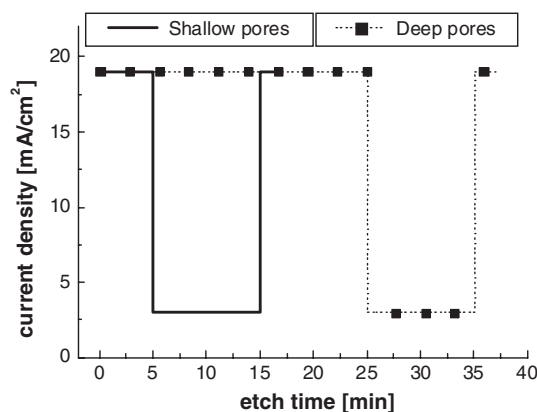


Figure 1. Current density curves versus etch time used to check for possible diameter modulation in shallow (solid line) and deep (points-dash line) pores.

Two different current densities versus etch time profiles were used. Profile 1: 19 mA/cm² for 5 min., 3 mA/cm² for 10 min., and finally 19 mA/cm² for 2 min. as shown in Figure 1, solid line. The resulting pores will be referred to as “shallow pores”. Profile 2: 19 mA/cm² for 25 min., 3 mA/cm² for 10 min., and finally 19 mA/cm² for 2 min. Figure 1, point-dash line, the resulting pores will be referred to as “deep pores”.

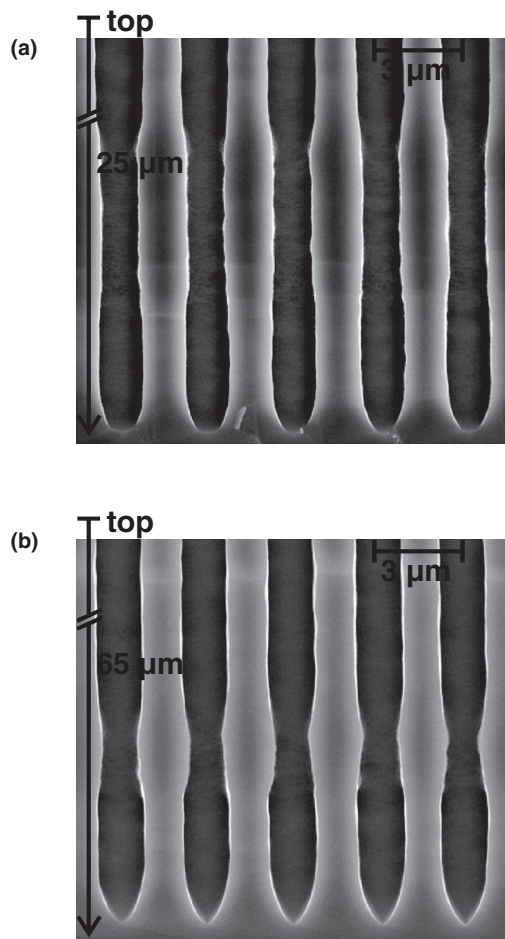


Figure 2. Scanning electron micrographs of macropores with modulated diameters using HF/DMF electrolyte. a) Shallow pores with a visible but not very pronounced reduction. b) Deep pores with pronounced diameter reduction.

FFT IS measurements were performed in-situ every 2 s. 24 frequencies in a range from 5 Hz to 20 kHz were employed in the impedance spectroscopy. A fully integrated laboratory etching system of ET&TE GmbH (Kiel, Germany) controlled all parameters of the etching procedure. The pore morphologies were examined by a SEM and compared to the FFT IS measurements for further analysis.

Results

Pore morphology and geometry.— Figure 2a shows pores etched with current density profile 1, using HF/DMF and achieving overall pore depths of approx. 25 μm. Figure 2b shows pores etched with current density profile 2, using HF/DMF and achieving overall pore depths of approx. 65 μm. Although the variation in the current density is the same, clearly the diameter modulation in Figure 2b is much stronger than in Figure 2a. Since the pore area scales with the square of the pore diameter, this is an even more pronounced difference for the variation of pore tip area. All experiments showed this trend: pore diameter modulations are easier in deeper pores, which is a first hint that some kind of diffusion limitation may be essential for large diameter modulation (and pore etching in general). Using the same current density profiles but changing the electrolyte to HF/DMF (PEG), diameter changes occur as shown in Figure 3. For the same over all etching time, pores are somehow shorter and slightly broader,

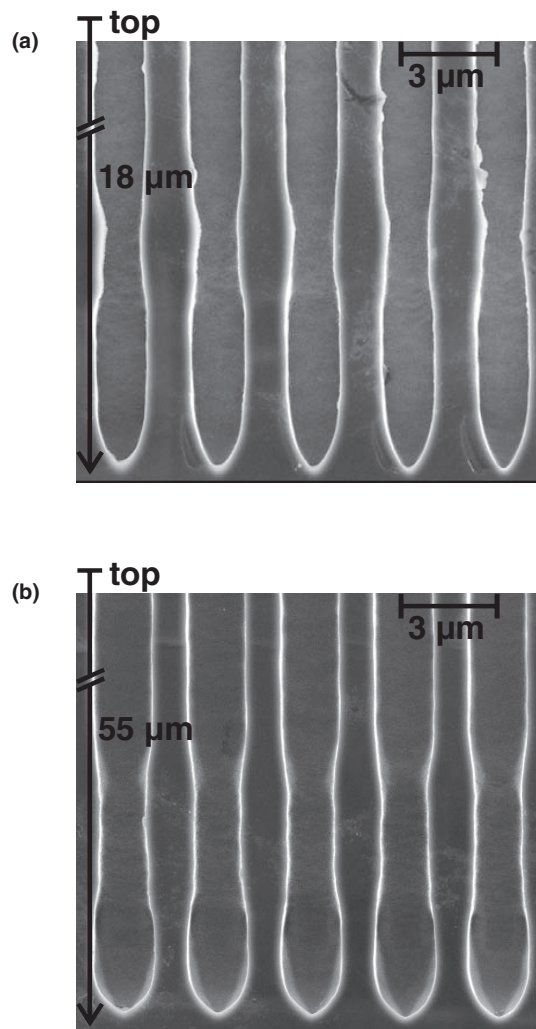


Figure 3. Scanning electron micrographs of macropores with modulated diameters using HF/DMF (PEG) electrolyte. a) Shallow pores with pronounced diameter variation. b) Deep pores with equally pronounced diameter variation.

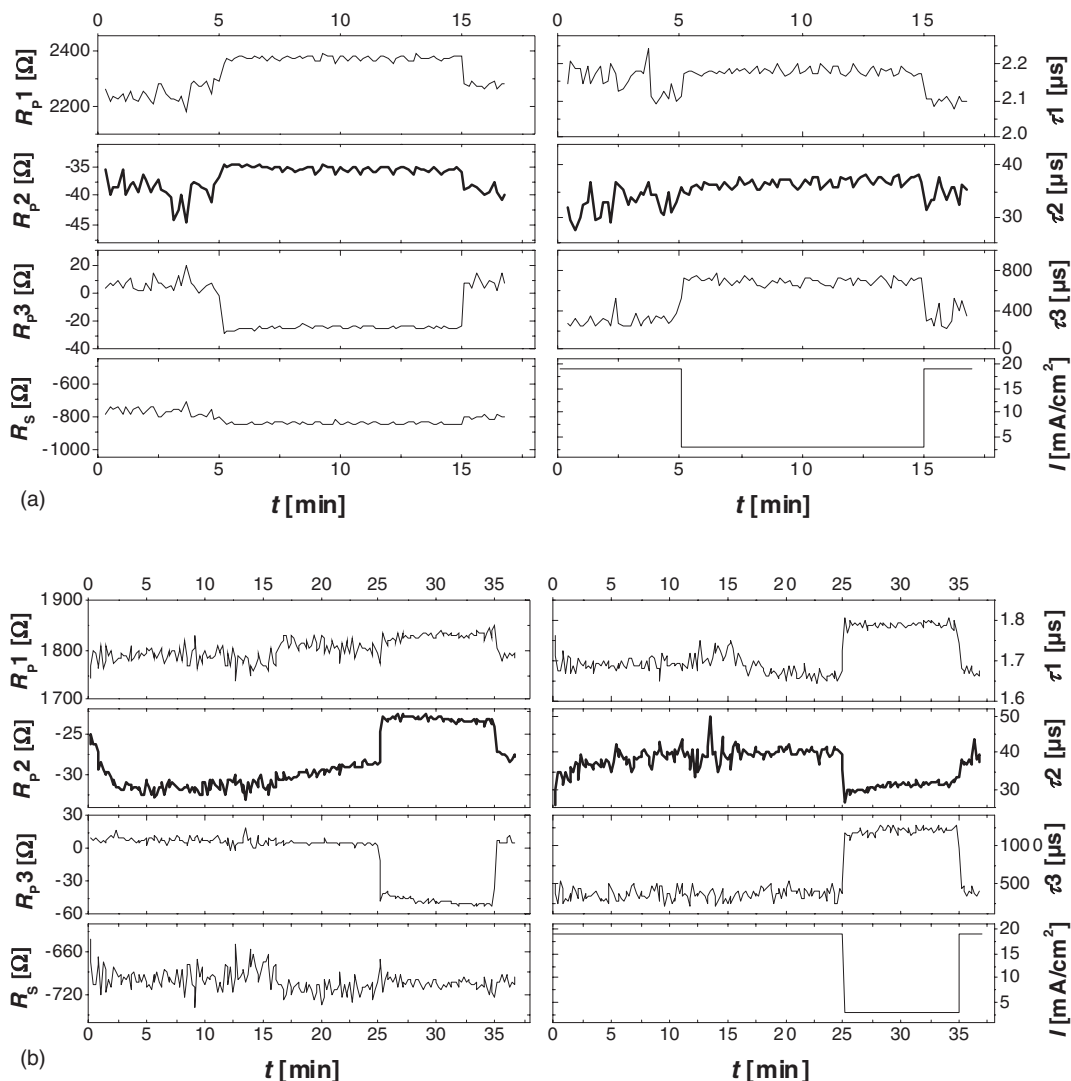


Figure 4. FFT IS data showing the behavior of the seven independent parameters with respect to current density and time using HF/DMF electrolyte. a) Shallow pores. R_s , τ_2 and R_{p2} stay almost constant, b) Deep pores. Apart from R_s , all the other parameters respond to the current density variation.

and shallow as well as deep pores show a more pronounced diameter variation. Since PEG has a high viscosity, the decrease in the etch rate can be attributed to an increased diffusion limitation. Within this set of experiments, clearly after the first pore diameter reduction the second diameter reduction was always much more pronounced and easier to achieve. Additionally, the PEG reduced the time for pore nucleation. Not all images of these experiments are shown here, but these experiments clearly suggest that a strong diffusion limitation is essential to allow for significant pore diameter modulation and more stable pore formation.

FFT IS results.— The FFT IS data for all conditions, i.e. high/low current density, with or without PEG, could be well fitted by simple equivalent circuit consisting of one series resistance R_s in series with three circuits in series, each one consisting of a resistor parallel to a capacitor $R_{pi}C_{pi}$. The FFT IS measurements thus comprise seven fitting parameters; here we use the 4 resistances and the three time constants $\tau_i = R_{pi}C_{pi}$. A detailed description of the in-situ FFT impedance analysis and the model used is given in.^{19–21} Figures 4 and 5 show the time dependence of the seven parameters plus the respective current density used for a particular experiment. The step like change in the current density is reflected in an instant change of almost all the fitting parameters.

In Figure 4a (shallow pores), one of the time constants τ_2 and the corresponding transient resistance R_{p2} stay almost constant, i.e. they do not respond to the variation of the current density. This impedance curves correspond to the pores shown in Figure 2a where no significant variation of the pore diameter was found.

The corresponding results for the electrolyte containing PEG are shown in Figure 5. Here a significant change is found for the time constant τ_2 and the corresponding transient resistance R_{p2} and these pores show a significant diameter variation. This obvious difference of process 2 for the experiments with and without PEG is reflected in the absolute numbers as well. While the other fitting parameters change roughly by a factor of two for the experiments with and without PEG, the time constant τ_2 as well as the transient resistance R_{p2} differ by at least one order of magnitude. For the long experiment using PEG from Figure 5b, one can see that after pore nucleation (which takes roughly 5 minutes), R_{p2} is decreasing with increasing pore length while R_{p1} is increasing with increasing pore length.

Using PEG, the slowest process 3 corresponding to the largest time constant τ_3 shows a continuous increase of the time constant τ_3 with increasing pore length (cf. Figure 5b). When reducing the current density in a step-like manner, the time constant τ_3 does not change instantaneously but relaxes slowly from large values to lower values. This means that process 3 needs some time to adapt to the drastically

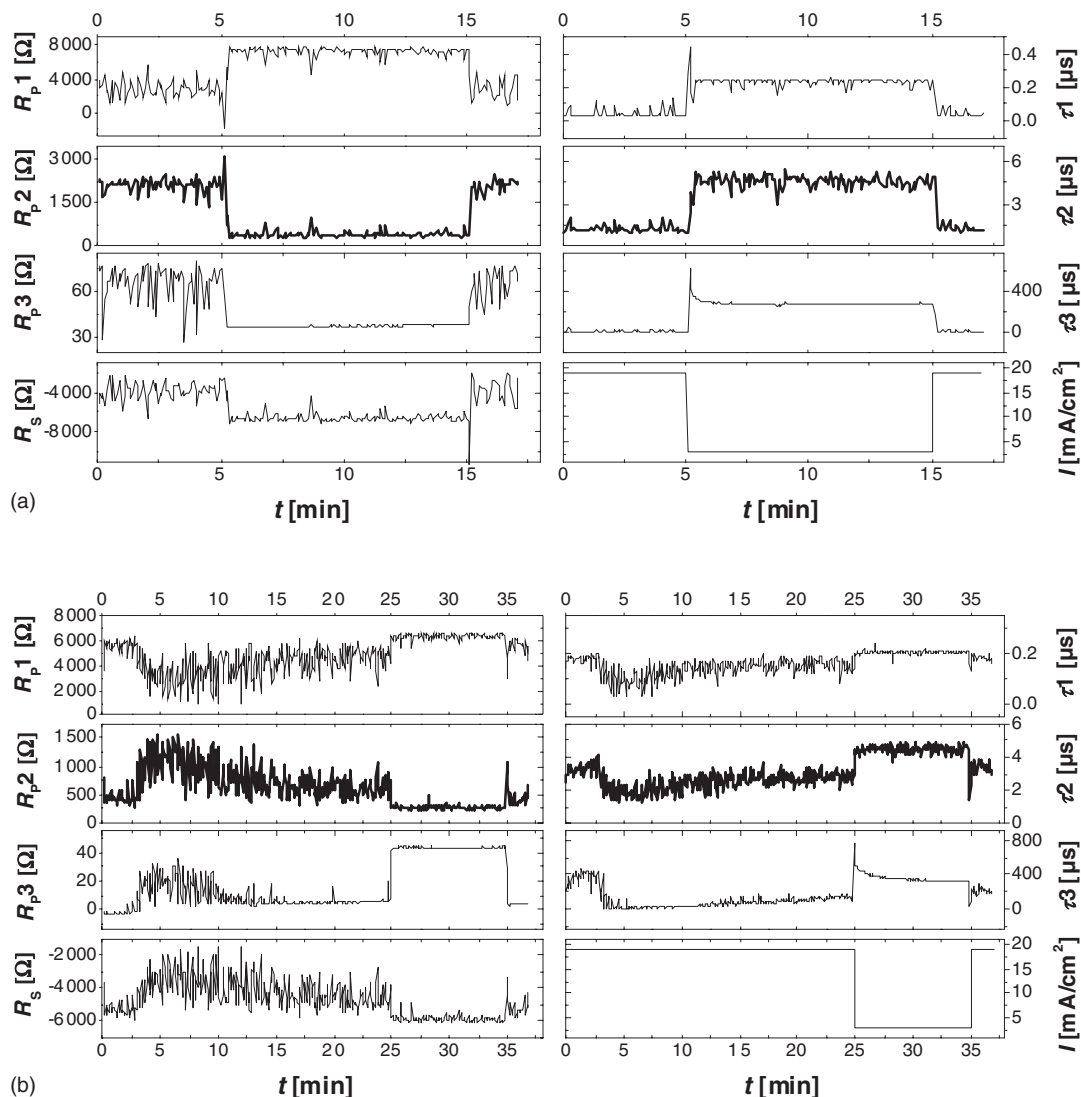


Figure 5. FFT IS data of samples etched using HF/DMF (PEG). All the seven independent parameters respond positively to the current density variation irrespective of the etch time. a) Shallow pores. b) Deep pores.

reduced current density. More details of the impedance curves could be discussed; here we mention only those effects that are common to other impedance data found in a series of similar experiments.

Discussion

The results for pore etching in p-Si presented in this paper only hold for pre-structured samples and low doped silicon, i.e. making the most of possible benefits from still present and overlapping space charge regions of neighboring pores that help to obtain sufficient selectivity for silicon dissolution between pore walls and pore tips. “Good” p-Si pore etching (i.e. long pores with smooth pore walls, constant diameter into the depth, not destroyed top part) quite obviously needs this feature much more than n-Si pore etching, where the back-side illumination is a second possibility for generating the selectivity. Overlapping space charge regions just reduce the applied anodic voltage across the pore wall - electrolyte interface and thus hinder electrochemical dissolution of the pore walls.

The results presented here can be understood if we assume that adding PEG to the HF/DMF electrolyte leads to a further reduction of pore wall dissolution or, in other words, a higher degree of passivation. PEG can improve pore formation on samples without pre-structured

nuclei as well, but it seems to need overlapping space charge regions to be really efficient. Essential for “good” pore etching are the following three processes:

1. easy dissolution of pore tips;
2. good passivation of pore wall, i.e. stability against dissolution;
3. efficient transition from the easily dissolved pore tip area to the passivated pore walls close to the tip and along the length of the pore.

The difference in dissolution between pore tip and pore walls often is called selectivity of dissolution. The third process is often ignored, but essential for understanding changes in pore diameter as a response to changes in the current density. In addition, this transition region is also instrumental for the often employed cavity formation by changing drastically the current density for deep pores.

All experimental results presented in this paper can consistently be understood when identifying the three processes in the above list as the processes described by the impedance fitting parameters R_{pi} and τ_i . The fastest process is most likely related to the dissolution of the pore tip, acting on the smallest area and thus showing the largest resistance although being most efficient. With increasing pore length the concentration of e.g. HF reduces at the pore tip and thus

leads to an increase of the resistance R_{p1} with increasing pore length. The second fastest process is most likely related to the over-all current through the pore walls, leading to a dissolution of the pore walls. With increasing pore length the over-all pore wall area increases, leading to a reduction of R_{p2} . The slowest process is most likely related to the current flowing in the transition area between pore tip and passivated pore walls. Adding PEG to the electrolyte drastically increases R_{p2} , which according to the model above, means a significant reduction of leakage current through the pore walls. Additionally, PEG reduces the time constant τ_3 , allowing for a faster “transition” from pore tip to pore wall. τ_3 was the only parameter showing a relaxation after step like reduction of the etching current density. Reducing the current density calls for a reduced pore tip area, which does not occur instantly but leads to the formation of a shoulder as visible in Figure 3. The length of this transition from a broad pore to a thin pore corresponds well to the transition time visible for τ_3 in Figure 5b.

The interpretation of the impedance data does not just take into account the result presented here but summarizes consistently other impedance data. e.g.^{8,15} In a nutshell, PEG leads to a much better and faster passivation of pore walls than just having overlapping space charge regions. Several papers state that adding PEG leads to much smoother pore walls in silicon.^{17,18} This is not only true for HF containing electrolytes but for KOH etching as well. So probably PEG acts in much the same way for p-Si pore formation as high acidic acid concentration acts in n-Si pore formation,²² leading to a quite consistent picture for the essences of anodic silicon pore etching.

Conclusions

Adding PEG to an HF/DMF electrolyte and using lithographically pre-structured low-doped p-type silicon deep pores with smooth pore walls, very “good” p-Si pores could be etched and even significant pore diameter modulations were possible by varying the current density. Comparing results with and without addition of PEG, especially using in-situ impedance data, three processes could be identified, two of which are significantly influenced by PEG. All results can be well

understood by assuming, that PEG leads to a more efficient and faster passivation of the pore walls.

Acknowledgments

This work was partly funded by the BMBF through the “AlkaSuSi” project under grant number 03X4618B.

References

1. V. Lehmann and H. Föll, *J. Electrochem. Soc.*, **137**(2), 653 (1990).
2. V. Lehmann and U. Grüning, *Thin Solid Films*, **297**, 13 (1997).
3. S. Matthias and F. Müller, *Nature*, **424**, 53 (2003).
4. S. Matthias, F. Mueller, J. Schilling, and U. Goesele, *Applied Physics A: Materials Science & Processing*, **80**, 1391 (2005).
5. H. Föll, M. Christophersen, J. Carstensen, and G. Hasse, *Mat. Sci. Eng. R*, **39**(4), 93 (2002).
6. M. Christophersen, J. Carstensen, S. Rönnebeck, C. Jäger, W. Jäger, and H. Föll, *J. Electrochem. Soc.*, **148**(6), E267 (2001).
7. A. Cojocar, J. Carstensen, and H. Föll, *ECS Trans.*, **16**(3), 157 (2008).
8. J. Carstensen, A. Cojocar, M. Leisner, and H. Föll, *ECS Trans.*, **19**(3), 355 (2009).
9. S. Matthias, F. Müller, C. Jamois, R. B. Wehrspohn, and U. Goesele, *Applied Physics A: Materials Science & Processing*, **16**, 2166 (2004).
10. J. Schilling, F. Müller, S. Matthias, R. B. Wehrspohn, U. Gösele, and K. Busch, *Appl. Phys. Lett.*, **78**, 1180 (2001).
11. E. K. Propst and P. A. Kohl, *J. Electrochem. Soc.*, **141**(4), 1006 (1994).
12. R. B. Wehrspohn, J.-N. Chazalviel, and F. Ozanam, *J. Electrochem. Soc.*, **145**, 2958 (1998).
13. M. Christophersen, J. Carstensen, A. Feuerhake, and H. Föll, *Mater. Sci. Eng. B*, **69–70**, 194 (2000).
14. J. Carstensen, M. Christophersen, and H. Föll, *Mat. Sci. Eng. B*, **69–70**, 23 (2000).
15. E. Ossei-Wusu, J. Carstensen, and H. Föll, *Nanoscale Res. Lett.*, **7**, 320 (2012).
16. J. Zheng, M. Christophersen, and P. L. Bergstrom, *Phys. Status Solidi A*, **202**(8), 1402 (2005).
17. V. Kochergin and H. Föll, *Porous Semiconductors: Optical Properties and Applications*, Springer, London (2009).
18. E. Quiroga-González, E. Ossei-Wusu, J. Carstensen, and H. Föll, *J. Electrochem. Soc.*, **158**(11), E119 (2011).
19. G. S. Popkurov and R. N. Schindler, *Rev. Sci. Instrum.*, **63**, 5366 (1992).
20. E. Foca, J. Carstensen, G. Popkurov, and H. Föll, *ECS Trans.*, **6**(2), 345 (2007).
21. J. Carstensen, E. Foca, S. Keipert, H. Föll, M. Leisner, and A. Cojocar, *Phys. Status Solidi A*, **205**(11), 2485 (2008).
22. E. K. Ossei-Wusu, A. Cojocar, J. Carstensen, M. Leisner, and H. Föll, *ECS Trans.*, **16**(3), 109 (2008).